Biogeochemistry **66:** 75–93, 2003.

Sources and fluxes of submarine groundwater discharge delineated by radium isotopes

WILLARD S. MOORE
Department of Geological Sciences, University of South Carolina, Columbia, SC 29208 (Phone: 803-777-2262 Fax: 803-777-6610)

Key words: Floridian aquifer, radium, submarine groundwater discharge, subterranean estuary

Abstract. This paper reports the results derived from radium isotopes of a submarine groundwater discharge (SGD) intercomparison in the northeast Gulf of Mexico. Radium isotope samples were collected from seepage meters, piezometers, and surface and deep ocean waters. Samples collected within the near-shore SGD experimental area were highly enriched in all four radium isotopes; offshore samples were selectively enriched. Samples collected from seepage meters were about a factor of 2–3 higher in radium activity compared to the overlying waters. Samples from piezometers, which sampled 1–4 meters below the sea bed were 1–2 orders of magnitude higher in radium isotopes than surface waters. The two long-lived Ra isotopes, ^{228}Ra and ^{226}Ra, provide convincing evidence that there are two sources of SGD to the study area: shallow seepage from the surficial aquifer and input from a deeper aquifer. A three end-member mixing model can describe the Ra distribution in these samples.

The short-lived radium isotopes, ^{223}Ra and ^{224}Ra, were used to establish mixing rates for the near-shore study area. Mixing was retarded within 3 km of shore due to a strong salinity gradient. The product of the mixing rate and the offshore ^{226}Ra gradient established the ^{226}Ra flux. This flux must be balanced by Ra input from SGD. The flux of SGD within 200 m of shore based on the ^{226}Ra budget was 1.5 m^3 min^{-1}. This flux agreed well with other estimates based on seepage meters and ^{222}Rn.

Introduction

Submarine groundwater discharge (SGD) is becoming acknowledged as an important flux of materials to the coastal ocean (Bugna et al. 1996; Cai & Wang 1998; Shaw et al. 1998; Moore 1999; Rutkowski et al. 1999; Burnett et al. 2002; Kelly & Moran 2002; Moore et al. 2002). Several components of SGD are recognized: (1) fresh water flowing directly from an aquifer to the ocean, (2) mixtures of fresh water and sea water cycling through surficial unconfined aquifers, and (3) inputs of freshwater-seawater mixtures from deeper semi-confined aquifers. These components may mix and react before

they enter the ocean. Ideally we would like to know the total flux of SGD to the coastal ocean and the fraction of this flux attributable to each of these three components. Chemical and radionuclide tracers offer promise in realizing this goal.

Moore (1999) reviewed the application of various radionuclide tracers to SGD studies. He concluded that the four naturally occurring radium isotopes are powerful tools to quantify SGD fluxes and to indicate the sources. The strategy for using radium isotopes in SGD studies is based on the fact that radium is largely particle-bound in fresh water but desorbs from particles in contact with salty water. Thus radium is especially useful for SGD studies where subsurface mixing of fresh and salty waters occur. The short-lived isotopes, ^{223}Ra (half life = 11.3 days) and ^{224}Ra (half life = 3.66 days), are continually regenerated from decay of their thorium parents, which are perpetually bound to particle surfaces. On the other hand the long-lived isotopes, ^{226}Ra (half life = 1600 yrs) and ^{228}Ra (half life = 5.7 yrs), require considerable time for regeneration. The differences in regeneration rates leads to differences in fluxes of each of these isotopes. For example if an aquifer has not been exposed to saline water for several thousand years, the ^{228}Ra/^{226}Ra activity ratio (AR) available to desorb will be close to the ^{232}Th/^{230}Th AR on the surface of the solids (normally in the range 0.5–1.5). But if the aquifer is continually flushed with saline water on a time scale of years, the ^{228}Ra/^{226}Ra AR will be high due to the more rapid regeneration of ^{228}Ra.

The short-lived Ra isotopes, ^{223}Ra and ^{224}Ra, constrain the mixing time of near-shore waters across the shelf. Offshore gradients of the long-lived Ra isotopes, ^{226}Ra and ^{228}Ra, coupled with the exchange rates from the short-lived isotopes, provide an estimate of Ra fluxes to the ocean. These fluxes must be sustained by input from rivers, sediments, SGD, or other sources. If we can measure or eliminate all other sources and establish the Ra concentration in the SGD, the Ra flux can be directly related to the SGD.

SGD intercomparison experiment

In August 2000 a SGD intercomparison experiment was organized by members of Scientific Committee on Oceanic Research (SCOR) Working Group 112 and the Land-Ocean Interaction in the Coastal Zone (LOICZ) project of IGBP (Burnett et al. 2002). The objective of this experiment was to compare estimates of SGD obtained from seepage meters (manual, heat pulse, and ultrasonic), geochemical tracers (^{226,228,223,224}Ra, ^{222}Rn, ^{3}H, ^{3}He, ^{4}He, and ^{14}C), and hydrologic modeling. The experiment was conducted in an area adjacent to the Florida State University Marine Laboratory (FSUML) on

the coastline of the northeast Gulf of Mexico during the period 13–18 August 2000.

The field site is located along an open shoreline within Apalachee Bay, a large embayment in the northeastern Gulf of Mexico, about 60 km south of Tallahassee, Florida. This area is known for significant near-shore seepage that is thought to originate from a surficial aquifer system and possibly from the main Floridan aquifer, which occurs just a few meters below the surface in this area. There is a wealth of background information from prior studies (Cable et al. 1996, 1997; Bugna et al. 1996; Rasmussen 1998; Rutkowski et al. 1999; Rasmussen et al. in press). The experimental design employed for the experiment consisted of two transects, set approximately 100 meters apart, consisting of piezometers and manual and automated seepage meters, arranged perpendicular to the shoreline out to about 200 m from shore. In addition to the piezometers and seepage meters, the area was instrumented with a continuous ^{222}Rn monitor and weather station. More details of the sampling site are available in Burnett et al. (2002) and Lambert et al. (this issue). Radium isotope samples were collected from this area and from an offshore cruise during the experiment. Additional samples were collected from the Ochlockonee River at the highway 319 bridge to the east of the study area and the New River to the west. An artesian well at the Parker Place campground adjacent to the New River was also sampled. Samples collected in the ocean above Lanark Spring in 1995 are also included. Lanark Spring is several km west of the experimental area. This paper reports the information gleaned from the radium isotope measurements.

Measurements

Nearshore samples (2–20 L) were collected from piezometers, seepage meters, an artesian well, creeks, and surface ocean waters. Offshore samples (150–200 L) were obtained during a cruise on the R/V Seminole. The cruise track extended about 28 km offshore (Figure 1). The outbound (eastern) leg was to the southeast of Dog Reef. The return (western) leg was to the west of the reef and southeast of Dog Island. Samples from the plume of Lanark Spring, about 10 km west of the SGD experimental area, were measured in 1995. Each sample volume was recorded and the water was pumped through a column of manganese coated acrylic fiber (Mn fiber) to quantitatively remove Ra (Moore 1976).

In the laboratory each Mn fiber sample was partially dried with a stream of air and placed in closed loop air circulation system described by Moore & Arnold (1996). Helium was circulated over the Mn fiber to sweep the ^{219}Rn and ^{220}Rn generated by ^{223}Ra and ^{224}Ra decay through a 1.1 L scintillation

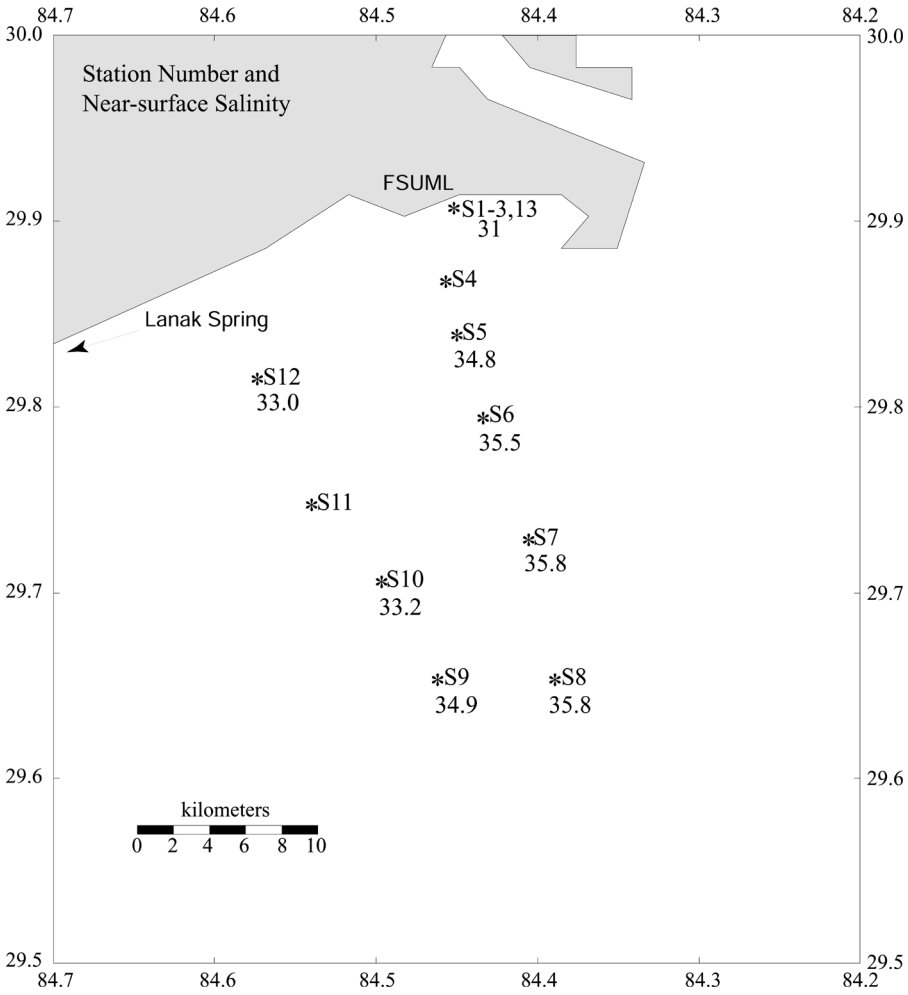

Figure 1. The distribution of salinity during the offshore cruise. Note the relatively low near-surface salinities at stations S9 and S10. Low salinities were also measured in the experimental seepage area near the shore.

cell where alpha particles from the decay of Rn and daughters were recorded by a photomultiplier tube (PMT) attached to the scintillation cell. Signals from the PMT were routed to a delayed coincidence system pioneered by Giffin et al. (1963) and adapted for Ra measurements by Moore & Arnold (1996). The delayed coincidence system utilizes the difference in decay constants of the short-lived Po daughters of ^{219}Rn and ^{220}Rn to identify alpha particles derived from ^{219}Rn or ^{220}Rn decay and hence to determine activities of ^{223}Ra and ^{224}Ra on the Mn fiber. The expected error of the short-lived Ra measurements is 10%.

After the ^{223}Ra and ^{224}Ra measurements were complete, the Mn fiber samples were aged for 2–6 weeks to allow initial excess ^{224}Ra to equilibrate with ^{228}Th adsorbed to the Mn fiber. The samples were measured again to determine ^{228}Th and thus to correct for supported ^{224}Ra.

Later, the Mn fibers were leached with HCl in a Soxhlet extraction apparatus to quantitatively remove the long lived Ra isotopes. The Ra was coprecipitated with $BaSO_4$. The precipitant was aged for 2 weeks to allow ^{222}Rn and its daughters to equilibrate with ^{226}Ra. The samples were measured in a gamma ray spectrometer to assess the activities of ^{226}Ra and ^{228}Ra (Moore 1984). The expected error of the long-lived Ra measurements is 7%.

Results

Samples collected within the SGD experimental area were unusually enriched in all four radium isotopes (Table 1). These enrichments, which are among the highest ever measured in nearshore waters, must be due to radium input from SGD because there is practically no surface water flow into this area and the underlying sediments are primarily quartz sand. Samples collected from seepage meters were about a factor of 2–3 higher in radium activity compared to the overlying waters (Table 1) with the exception of sample S1, which was similar in activity to the water from the seepage meters. Samples from piezometers were 1–2 orders of magnitude higher than surface waters (Table 1). These piezometers sampled groundwaters 1–4 meters below the sea-bed at various distances from shore.

Figure 1 shows the station numbers for the offshore cruise and the salinity at 1–2 m depth. Note the relatively low salinity at stations S9 and S10. At most offshore stations a CTD cast was used to determine the structure of the water column. During earlier studies (Cable et al. 1996) the offshore waters were characterized by a strong thermocline that effectively isolated the deeper waters from the surface. The thermocline was not present during this investigation. Figure 2 shows the salinity as a function of depth at stations with CTD measurements. The surface water at stations S9, 10, and 12 are significantly fresher compared to other offshore stations. This freshening extends to the bottom at station S10. The water column at station S10 was about 1 °C cooler than the other stations (Table 1). Unfortunately the CTD failed at S11.

The distribution of each radium isotope on the Seminole cruise and in the surface water at the piezometer and seepage site is shown in Figure 3. Surface waters sampled during the eastern leg of the cruise showed a rather consistent decrease in radium isotopes with the exception of the most seaward station (S8), which had slightly higher activities of the long-lived isotopes. A depth profile at station 8 had the same activity of ^{226}Ra through the water

Table 1. Radium samples from intercomparison experiment. All activities are dpm/100L

Sample	Depth m	Collection date	Temp. °C	Salinity	^{226}Ra	^{228}Ra	^{223}Ra	ex^{224}Ra	^{228}Th
Open water samples									
S1	1	14-Aug-00		31.74	70.8	137.3	35.76	146.4	5.9
S2	1	14-Aug-00			42.9	113.7	40.34	141.0	6.4
S3	1	14-Aug-00			37.7	65.6	23.25	86.9	4.8
S4	5	15-Aug-00			24.4	51.8	8.56	39.5	2.4
S5	5	15-Aug-00	29.82	34.81	14.9	23.8	5.06	25.7	1.4
S6	5	15-Aug-00	30.66	35.51	12.8	19.1	4.16	15.0	1.4
S7	5	15-Aug-00	30.27	35.82	12.7	15.1	2.63	8.3	1.1
S8	5	15-Aug-00	29.97	35.75	14.1	21.9	1.70	3.9	1.0
S8	10	15-Aug-00	30.04	36.03	12.8	13.6	1.82	4.5	0.9
S8	19	15-Aug-00	30.05	36.00	14.9	23.9	2.38	5.3	1.8
S9	5	15-Aug-00	30.05	35.74	26.8	30.7	2.91	8.6	1.1
S10	5	15-Aug-00	29.03	33.47	22.9	30.2	3.23	12.6	1.4
S10	13	15-Aug-00	29.00	33.57	22.5	26.1	2.61	8.7	1.2
S11	5	15-Aug-00			19.6	29.6	0.85	3.5	
S12	5	15-Aug-00	30.40	34.90	16.2	25.9	1.08	3.6	
S13	1	16-Aug-00			41.8	100.4	34.04	108.7	7.9
Piezometers									
FC-D1	4.6	14-Aug-00		26.74	6458	2201	368	267400	82
FC-C3	1.2	14-Aug-00		32.28	176	646	265	322800	40
FC-C1	3.7	14-Aug-00		23.95	1554	2687	526	239500	126
FC-BC1	3.8	14-Aug-00		20.00	1129	709	494	200000	46
FC-B4	1.0	14-Aug-00		24.00	6292	1559	1190	240000	102
FC-AB1	3.5	14-Aug-00		30.00	62	100	16	0	7
FC-A3	1.9	14-Aug-00		0.57	83	103	23	5700	40
Seep meters									
FC-KC		16-Aug-00		31.77	76	140	82	317700	7
FC-Y1		16-Aug-00		31.82	92	156	119	318200	10
Rivers & wells									
FC-OR		16-Aug-00		0.25	41	53	71	4	2
FC-NR		16-Aug-00		0.09	35	41	146	13	2
FC-AW		16-Aug-00		0.29	201	91	724	69	3
FSUML GW		11-Dec-95		0.22	778	142			
Lanark Spring 1995									
LS-B	1	3-Nov-95			53.8	50.1	14.2	32.8	
LS-20-D	1	3-Nov-95			52.5	44.1	12.8	37.8	
LS-50-D	1	3-Nov-95			59.6	50.2	9.8	38.3	
LS-100-U	1	3-Nov-95			45.7	36.1	6.0	28.5	

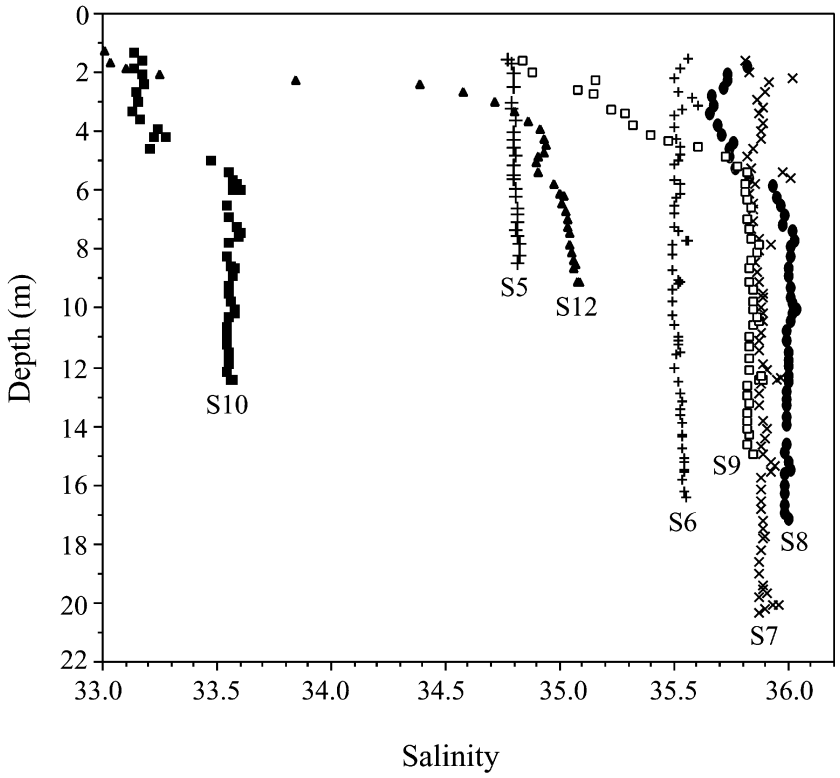

Figure 2. Salinity at each station was measured as a function of depth. Note that the surface water at stations S9, 10, and 12 are significantly fresher compared to other stations.

column, but slightly lower ^{228}Ra at mid depth. Activities of the short-lived isotopes were higher in the bottom water compared to the surface at this station. The western leg was quite different from the eastern leg. On the western leg the highest activities of all radium isotopes occurred at the two stations farthest from shore. At the second station (S10), activities of the two long-lived isotopes were similar in surface and bottom waters, but the short-lived isotopes were both higher in the surface waters. It is apparent that recent inputs of radium >20 km from shore impacted the outermost stations on the western leg. The radium added offshore had a lower ^{228}Ra/^{226}Ra AR than the trend from the eastern leg of the cruise (Figure 4). These offshore samples fall close to a mixing trend with samples from Lanark Spring and the onshore Parker Place artesian well adjacent to the New River.

Samples from the Ochlokonee River (FC-OR) and New River (FC-NR) were similar in ^{226}Ra and ^{228}Ra activity to ocean samples from the seepage area. This does not imply that these rivers are a significant source of radium

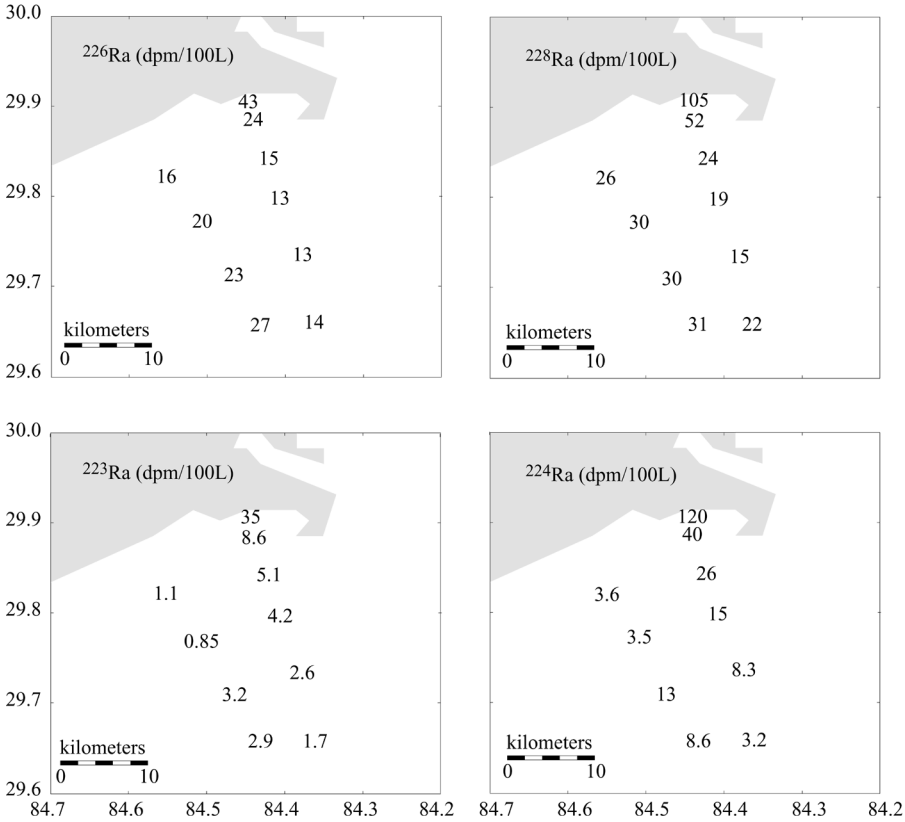

Figure 3. The distribution of radium isotopes in surface waters. Note the high activities of all radium isotopes at the two stations farthest from shore on the western transect.

to the coastal area because the radium concentration would be diluted by over a factor of 100 as the river water mixed with ocean water to attain the salinity of the coastal ocean. Desorption of radium from particles carried by these rivers is likewise a minor source of radium to the study area due to dilution.

Discussion

Radium sources

The ^{226}Ra and ^{228}Ra activities in samples collected in the experimental seepage area are among the highest that have been measured in ocean water samples. These high activities decrease considerably for samples collected offshore. The consistent ^{228}Ra/^{226}Ra AR for samples collected in the seepage

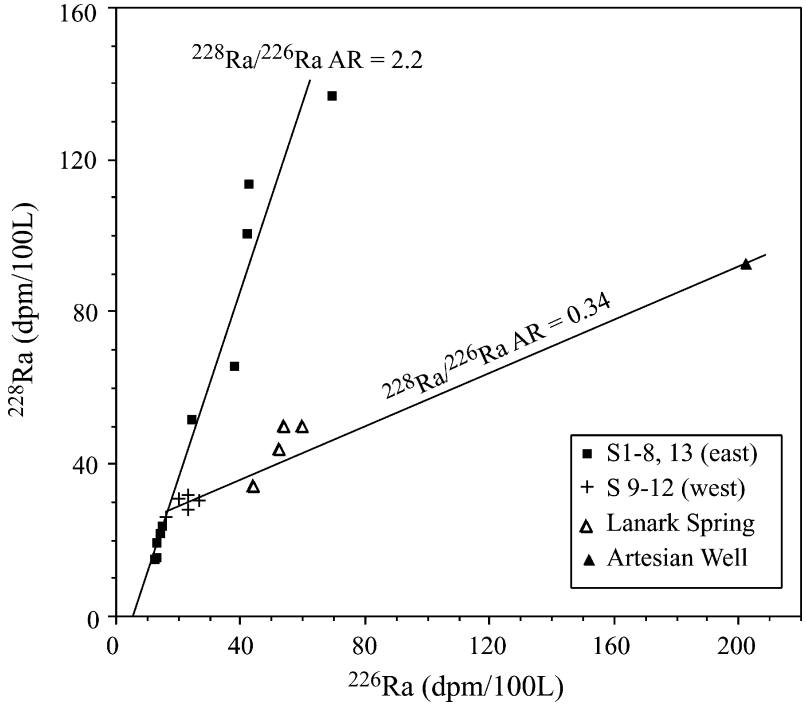

Figure 4. The distribution of ^{228}Ra and ^{226}Ra reveals two trends, one for the nearshore samples and samples from the eastern transect, another for the western transect, Lanark Spring, and the Parker Place artesian well. This implies there are two sources of radium.

area and on the eastern leg of the cruise (Figure 4) implies that the radium in these samples has a unique source. This source is likely the waters sampled by piezometers on the "C" transect (Figure 5). Samples from the shallow piezometer C3 (depth = 1 m below the seabed, salinity = 32) and C1 (depth = 3.5 m, salinity = 24) fall near the ^{228}Ra-^{226}Ra mixing line defined by ocean samples from the SGD area and the eastern leg of the offshore cruise (Figures 4 and 5). Samples from the other piezometer transects have considerably lower ^{228}Ra/^{226}Ra AR's. A fresh water sample from the Marine Lab well (FSUML GW) also falls close to this lower AR line. Had the Ra in the nearshore water been derived primarily from these sources, the nearshore AR would have been much lower. There is a suggestion that some near-shore samples may contain a component with a lower ^{228}Ra/^{226}Ra AR.

At some of the offshore stations on the western transect, temperature, salinity, and radium data indicate a substantial input of SGD >20 km from shore. Station S10 has a significantly lower temperature and salinity than the other stations (Table 1) implying the recent input of cooler, fresher water. The

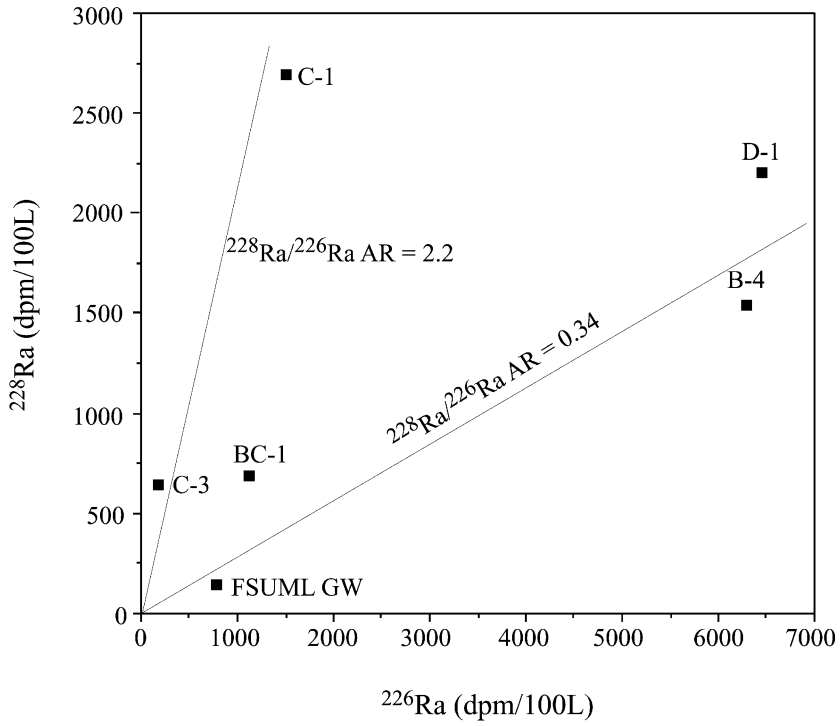

Figure 5. Extension of the trends noted on Figure 4 intersect different piezometer samples, reinforcing the conclusion of two radium sources.

presence of high activities of the short-lived Ra isotopes at selected stations 20 km from shore (Figure 3) requires that the input occurred shortly before the samples were collected or the input was continuing as we sampled. If the input had occurred more than several days before the cruise and ceased, the temperature, salinity, and radium isotope signals would have merged with the surrounding ocean. Instead these signals stand out as a cool, low salinity plume, rich in short-lived Ra isotopes. Moore & Shaw (1998) reported high activities of radium isotopes in samples collected on the continental shelf 40–80 km from Charleston, SC, in water depths of 20–45 m. Subsequent cruises to this area have not found such high activities (Moore in prep).

The lower salinity and temperature in the offshore plume suggest that the source of the input is SGD from a semi-confined aquifer on the shelf. The low $^{228}Ra/^{226}Ra$ AR in the offshore plume indicates that the deeper aquifer is flushed more slowly than the nearshore aquifer, that the $^{232}Th/^{230}Th$ AR of the solids is lower, or both. The samples from the low salinity plume fall near a low $^{228}Ra/^{226}Ra$ AR mixing line that also includes the samples from Lanark Spring and the Parker Place artesian well (Figure 4). Samples from

the FSUML well and the B-4 piezometer also fall close to this low AR line (Figure 5).

The long-lived Ra isotopes may be used to estimate the relative SGD inputs to the study area from the nearshore high AR and offshore low AR sources. The sample from the C3 piezometer will be used to characterize the nearshore end-member or source term and the artesian well will be used to characterize the input from the deep offshore aquifer. The following equations will be used to establish a 3-end-member mixing model.

$$f_o + f_{ns} + f_{os} = 1.00 \tag{1}$$

$$^{226}Ra_o f_o + {}^{226}Ra_{ns} f_{ns} + {}^{226}Ra_{os} f_{os} = {}^{226}Ra_m \tag{2}$$

$$^{228}Ra_o f_o + {}^{228}Ra_{ns} f_{ns} + {}^{228}Ra_{os} f_{os} = {}^{228}Ra_m \tag{3}$$

where

f is the fraction of ocean (o), nearshore SGD (ns), or offshore SGD (os) end-member,

Ra_o is ^{226}Ra or ^{228}Ra activity in the ocean end-member,

Ra_{ns} is ^{226}Ra or ^{228}Ra activity in the nearshore SGD end-member,

Ra_{os} is ^{226}Ra or ^{228}Ra activity in the offshore SGD end-member,

Ra_m is measured ^{226}Ra or ^{228}Ra activity in the sample.

These equations may be solved for the fractions of each end-member.

$$f_{ns} = \frac{\left[\frac{^{228}Ra_m - {}^{228}Ra_o}{^{228}Ra_{os} - {}^{228}Ra_o}\right] - \left[\frac{^{226}Ra_m - {}^{226}Ra_o}{^{226}Ra_{os} - {}^{226}Ra_o}\right]}{\left[\frac{^{228}Ra_{ns} - {}^{228}Ra_o}{^{228}Ra_{os} - {}^{228}Ra_o}\right] - \left[\frac{^{226}Ra_{ns} - {}^{226}Ra_o}{^{226}Ra_{os} - {}^{226}Ra_o}\right]} \tag{4}$$

$$f_{os} = \frac{^{228}Ra_m - {}^{228}Ra_o - f_{ns}\left[^{228}Ra_{ns} - {}^{228}Ra_o\right]}{^{228}Ra_{os} - {}^{228}Ra_o} \tag{5}$$

$$f_o = 1.00 - f_{ns} - f_{os} \tag{6}$$

For the ocean end-member we use the data of Reid & Sackett (1982); ^{226}Ra = 9 dpm/100L and ^{228}Ra = 4 dpm/100L. These samples were collected from the central Gulf of Mexico 20 years earlier. For the nearshore SGD end-member we use the sample from piezometer C3 (FC-C3), ^{226}Ra = 176 dpm/100L and ^{228}Ra = 646 dpm/100L. For the deep offshore SGD end-member we use the sample from the onshore artesian well (FC-AW), ^{226}Ra = 201 dpm/100L and ^{228}Ra = 91 dpm/100L. Table 2 gives the results of the model. All of the samples can be represented by these 3 end-members. The values used for the end-members represent an approximation based on very limited sampling. If the sample from piezometer C1 (FC-C1) is used for the nearshore end-member, the model produces negative numbers for many of the

Table 2. Results of mixing model to separate SGD from near-shore and offshore aquifers. Activities are dpm/100L

Station	Depth m	Distance offshore, km	$^{226}Ra_m$	$^{228}Ra_m$	f_{ns}	f_{os}	f_o
Near-shore							
S1	1	0.1	70.81	137.32	0.19	0.16	0.65
S2	1	0.1	42.92	113.70	0.17	0.03	0.80
S3	1	0.1	37.73	65.56	0.09	0.08	0.84
S13	1	0.1	41.84	100.44	0.14	0.05	0.81
Lanark Spring	1	0.2	59.60	50.20	0.04	0.23	0.73
Eastern transect							
S4	5	3	24.40	51.76	0.07	0.02	0.91
S5	5	8	14.91	23.84	0.03	0.00	0.97
S6	5	12	12.85	19.15	0.02	0.00	0.98
S7	5	19	12.68	15.05	0.02	0.00	0.98
S8	5	27	14.12	21.88	0.03	0.00	0.97
S8	10	27	12.78	13.57	0.01	0.01	0.98
S8	19	27	14.89	23.89	0.03	0.00	0.97
Western transect							
S9	5	27	26.75	30.68	0.03	0.06	0.90
S10	5	20	22.88	30.17	0.04	0.04	0.92
S10	13	20	22.51	26.05	0.03	0.05	0.93
S11	5	13	19.59	29.56	0.04	0.02	0.94
S12	5	7	16.16	25.95	0.03	0.01	0.96

Ra_m – Ra measured, f_{ns} – fraction of near-shore aquifer, f_{os} – fraction of offshore aquifer, f_o – fraction ocean water.

components, implying that this is not an appropriate end-member. The goal here is to demonstrate that three end-members can describe the Ra activity. As the end-members are better defined through future work, the model can be tuned.

An unexpected result of the model is the presence of a significant and variable deep aquifer component in the nearshore samples. Samples from the offshore eastern transect retain a small component of the near-shore aquifer, but are not significantly influenced by offshore discharge from the deep aquifer. Samples from the western transect are significantly influenced by the deeper aquifer. Samples from Lanark Spring are likewise strongly influenced by the deep aquifer.

To estimate the seepage rate of groundwater into the study area, I use the approach developed earlier (Moore 1996, 2000). This approach first establishes the offshore mixing rate of the study area and the offshore ^{226}Ra gradient. The product of these terms is the offshore ^{226}Ra flux. If the system is steady state, the offshore ^{226}Ra flux must be supported by a SGD flux enriched in ^{226}Ra. Dividing the offshore ^{226}Ra flux by the activity of ^{226}Ra in the groundwater yields the SGD flux.

The change in concentration or activity (A) with time (t) as a function of distance offshore (x) for a radioactive tracer with decay constant (λ) may be expressed as a balance of advection, dispersion, and decay

$$\frac{dA}{dt} = K_h \frac{\partial^2 A}{\partial x^2} - \omega \frac{\partial A}{\partial x} - \lambda A \tag{7}$$

If net advection can be neglected, this reduces to

$$\frac{dA}{dt} = K_h \frac{\partial^2 A}{\partial x^2} - \lambda A \tag{8}$$

where K_h is the eddy mixing coefficient. In this case the boundary conditions are

$$A = A_i \text{ at } x = 0$$
$$A \to 0 \text{ as } x \to \infty$$

If K_h is constant and the system is steady state,

$$A_x = A_0 \exp\left[-x\sqrt{\frac{\lambda}{K_h}}\right] \tag{9}$$

where

A_x = activity at distance x from coast
A_0 = activity at distance 0 from coast
λ = decay constant

A plot of ln ^{223}Ra or ln ^{224}Ra as function of distance from the coast may be used to estimate K_h if the exchange is dominated by eddy diffusion rather than advection and if the system is steady state.

$$\ln A_x = \ln A_0 - x\sqrt{\frac{\lambda}{K_h}} \tag{10}$$

$$\text{In this case the slope, } m = \sqrt{\frac{\lambda}{K_h}} \tag{11}$$

Surface samples from the eastern transect were not significantly influenced by the offshore discharge. Because these samples represent primarily mixing between the nearshore and ocean end-members, we can use the eddy mixing model based on the short-lived Ra isotopes to estimate the rate of mixing. Figure 6 shows the activities of the ln transforms of ^{223}Ra and ^{224}Ra as a function of distance from shore for samples from the SGD experimental area and the eastern leg of the cruise. Two curves are apparent on each plot, one from 0–3 km offshore and another from 3–27 km offshore. The clear break in slope at about 3 km from shore indicates slower mixing nearshore compared to the rates further offshore. The nearshore-offshore differences probably reflect a strong horizontal density gradient due to the presence of fresher (31 ppt) water nearshore and saltier water (35 ppt) offshore. Had we anticipated this difference in mixing rates, we would have collected more nearshore samples. Although the present data set is far from ideal, it does allow an illustration of how to approach the problem. This work is continuing.

For ln ^{223}Ra the distribution within 3 km of shore has a slope of –0.518 km^{-1} with R^2 = 0.950. The distribution of ln ^{224}Ra over the same interval has a slope of –0.425 km^{-1} with R^2 = 0.903. Using equation 11 and its assumptions, the value of K_h derived from ^{223}Ra is 0.23 km^2 d^{-1} (2.7 m^2 s^{-1}); ^{224}Ra yields K_h = 1.0 km^2 d^{-1} (12 m^2 s^{-1}). The differences in these estimates may be due in part to differences in the time and space scales of eddy mixing. The longer lived ^{223}Ra looks at a larger scale than ^{224}Ra. There are also analytical difficulties in the ^{224}Ra measurement that do not affect the ^{223}Ra measurement. High activities of ^{228}Ra in the water produce ^{228}Th, the parent of ^{224}Ra. Thorium is scavenged by the Mn-fiber during sample collection. Because these samples were not measured until about one half of the excess ^{224}Ra had decayed, the correction for ingrowth from ^{228}Th on the fiber is significant. Thus the ^{224}Ra data are not as accurate as the ^{223}Ra data; this is reflected in the poorer fit of the ^{224}Ra data to the model.

We may use the parameters derived here to calculate the flux of ^{226}Ra from near the coast to the ocean. The flux of a conservative tracer can be estimated from the product of the offshore concentration gradient and K_h. The ^{226}Ra gradient is –6.43 dpm 100L^{-1} km^{-1} or –6.43 x 10^{10} dpm km^{-3} km^{-1} (Figure 7). Again, the sampling density is not ideal. One sample (FC-S1) with an anomalous high ^{226}Ra activity and strong deep aquifer influence has been omitted. For K_h = 0.23 km^2 d^{-1} (based on the ^{223}Ra estimate), the offshore ^{226}Ra flux is 1.5 x 10^{10} dpm km^{-2} d^{-1}. In this case km^{-2} refers to a vertical cross-section area parallel to the coast. This Ra is transported offshore from the experimental SGD site, which is 1.3 m deep and 100 m wide (vertical cross-section area = 1.3 x 10^{-4} km^2). Therefore, the offshore flux from the experimental SGD site is 1.9 x 10^6 dpm d^{-1}. If the ^{226}Ra activity in water

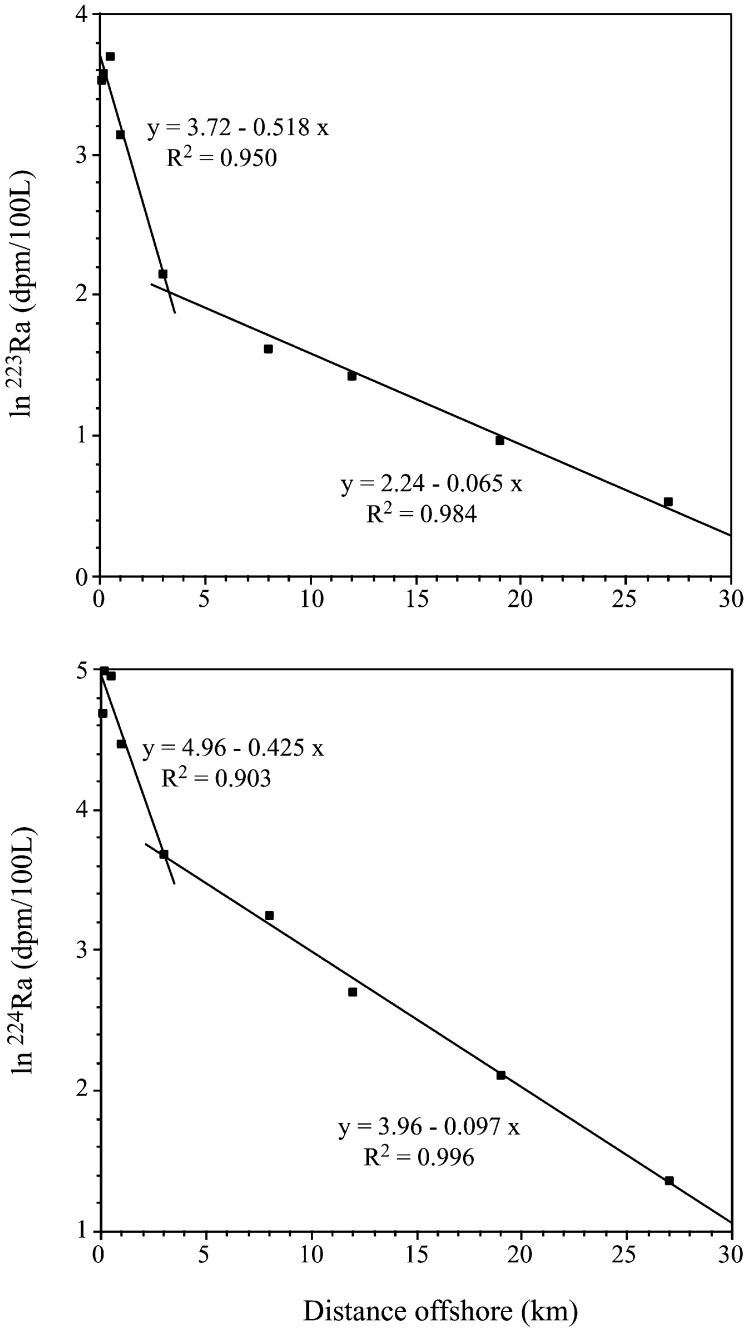

Figure 6. The ln transforms of ^{223}Ra and ^{224}Ra activity as a function of distance from shore are used to estimate mixing rates. The two curves indicate slower mixing nearshore compared to the rates further offshore.

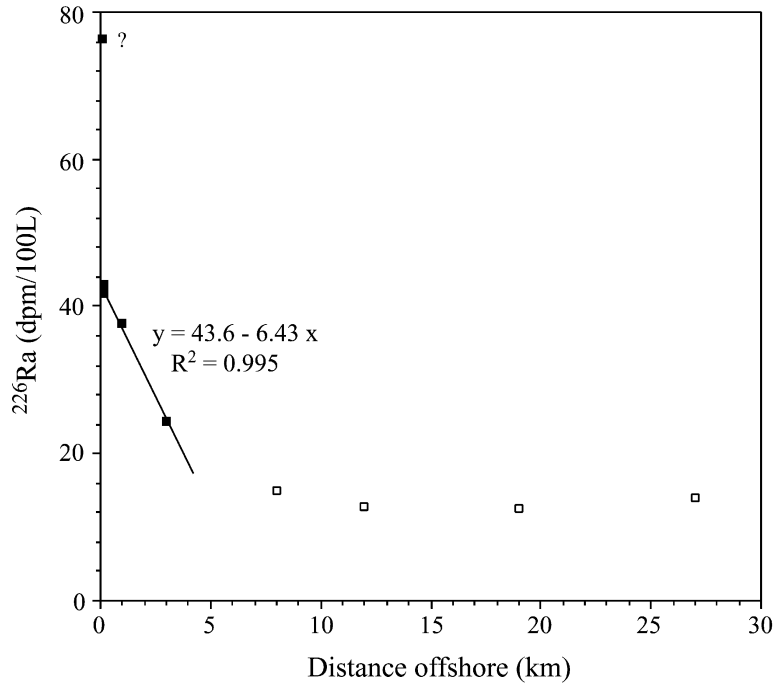

Figure 7. The 0–3 km offshore ^{226}Ra gradient is –6.43 dpm 100L^{-1} km^{-1}. This is based on samples shown as filled squares.

collected in the Y-1 seepage meter (0.92 dpm L^{-1}) represents the average SGD flux into the study area, the amount of SGD required to support the offshore ^{226}Ra flux is 2.1 x 10^{6} L d^{-1} or 1.5 m^{3} min^{-1}. This represents the entire seepage over the experimental site. Burnett et al. (2002) and Lambert et al. (this issue) have noted that most of this seepage occurs within 100 m of shore.

There are other ways to interpret the data. Had I used the K_h based on the ^{224}Ra profile, the seepage rate required would be about 4 times greater. As noted earlier K_h based on the ^{223}Ra gradient is probably a more accurate measure of mixing in this case. ^{228}Ra could also be used to calculate fluxes and SGD. However, the nearshore ^{228}Ra gradient is not as well defined as ^{226}Ra. Why this is the case is uncertain. The choice of the ^{226}Ra activity of the SGD also influences the calculated fluxes. Using water sampled by the C3 piezometer (1.76 dpm/L) instead of that collected in the Y-1 seepage meter, would reduce the water flux by a factor of 1.9. I used Y-1 because this is the SGD that is actually reaching the ocean. The difference between Y-1 and C3 must represent the amount of local sea water entrainment as the water travels from 1 m depth to the surface. Rasmussen et al. (in press) modeled the

advection of SGD at this site and concluded that small-scale convection cells cause considerable mixing of sea water and meteoric water in the shallow sediments.

Seepage meters and ^{222}Rn modeling in the nearshore zone estimated discharge rates of 1.6 to 2.5 m^3 min^{-1} for the 2 x 10^4 m^2 study area (Burnett et al. 2002). The near-shore SGD fluxes estimated from the radium isotope measurements agree well with these estimates. In addition to the reservations outlined above, several caveats must be recognized in the Ra-based estimates. We have not established that the system is steady state. Repeated tidally-averaged measurements over an extended period would be required to make this determination. The ^{223}Ra gradient from shore to 3 km was much sharper than expected and sampling was not optimal to resolve the gradient. The true gradient could be greater than measured. On the other hand due to the lack of stratification, the nearshore ^{223}Ra flux is mixed into deeper water (from 1.3 to 6 m) as it moves offshore. This dilution decreases the ^{223}Ra concentration at 3 km and thus increases the apparent gradient within the first 3 km. We do not know how closely these effects offset each other. There are similar considerations in the case of ^{226}Ra that may affect its true gradient. Additionally, one anomalous high ^{226}Ra value was excluded from the calculation. If the true ^{223}Ra gradient is more negative than measured, the mixing rate will be lower than we have estimated. This would imply that the ^{226}Ra flux is less than estimated. But, if the ^{223}Ra is more negative than measured, the true ^{226}Ra gradient is probably more negative as well. Thus, the product of the mixing rate and ^{226}Ra gradient will be affected less than either individual term. Since the product is used to derive the radium and hence the water flux, the estimates made here may be more reliable than the caveats indicate. These estimates of SGD are certainly not the last word on the subject; future work must focus more attention on sampling nearshore where most of the changes occurred.

Conclusions

This study has demonstrated the utility of the four radium isotopes in identifying the sources of submarine groundwater discharge and (with reservations) quantifying some of these sources. The sources to this study area were the surficial aquifer, which discharged within 100 m of the coast, and a deeper aquifer, which discharged near shore and at least 28 km from shore. Using the distributions of the short-lived radium isotopes, near-shore mixing rates were calculated. The product of the offshore ^{226}Ra gradient and the mixing rate is the offshore ^{226}Ra flux required to sustain the gradient. Dividing the ^{226}Ra flux by the concentration of ^{226}Ra in seepage waters,

yields the SGD. In this experiment SGD calculated from the radium balance matched closely that measured in seepage meters and modeled from the ^{222}Rn distribution.

The presence of multiple groundwater sources to this region complicates the assessment of the effects of SGD. The different sources may have different concentrations of nutrients, carbon, metals, and fresh water. To properly evaluate the effects of SGD, each groundwater source must be evaluated with respect to its flux and concentration of materials of interest. Workers in other areas should be alert to the possibility of multiple groundwater sources.

Acknowledgments

I thank Bill Burnett for providing the logistical support for this experiment and for discussions that improved the manuscript. Ann Mulligan, Jaye Cable, Guebuem Kim, Mike Lambert, and Jamie Christoff assisted in sample collections. Melanie Doyle assisted in the lab. Three reviewers suggested changes that improved the manuscript. Working Group 112, "Magnitude of Submarine Groundwater Discharge and its Influence on Coastal Oceanographic Processes," was sponsored by SCOR and LOICZ. SCOR is funded in part by the National Science Foundation under Grant No. 0003700. This research was supported by NSF grant OCE-97-12298.

References

Bugna GC, Chanton JP, Young JE, Burnett WC & Cable PH (1996) The importance of groundwater discharge to the methane budgets of nearshore and continental shelf waters of the northeastern Gulf of Mexico. Geochim. Cosmochim. Acta 60: 735–4746

Burnett WC, Chanton J, Christoff J, Kontar E, Krupa S, Lambert M, Moore W, O'Rourke D, Paulsen R, Smith C, Smith L & Taniguchi M (2002) Assessing methodologies for measuring groundwater discharge to the ocean. EOS 83: 117–123

Cable JE, Burnett WC, Chanton JP & Weatherly GL (1996) Estimating groundwater discharge into the northeastern Gulf of Mexico using radon-222. Earth Planet. Sci. Lett. 144: 591–604

Cable JE, Burnett WC, Chanton J, Corbett DR & Cable P (1997) Field evaluation of seepage meters for coastal marine work. Estuar. Coast. Shelf Sci. 45: 367–375

Cai W-J & Wang Y (1998) The chemistry, fluxes, and sources of carbon dioxide in the estuarine waters of the Satilla and Altamaha Rivers, Georgia. Limnol. Oceanog. 43: 657–668

Giffin C, Kaufman A & Broecker WS (1963) Delayed coincidence counter for the assay of actinon and thoron. J. Geophys. Res. 68: 1749–1757

Kelly RP & Moran SB (2002) Seasonal changes in groundwater input to a well-mixed estuary estimated using radium isotopes and implications for coastal nutrient budgets. Limnol. Oceo. 47: 1796–1807

Lambert MJ & Burnett WC (2003) Submarine groundwater discharge estimates at a Florida coastal site based on continuous radon measurements. Biogeochemistry: this issue

Moore WS (1976) Sampling radium-228 in the deep ocean. Deep-Sea Res. 23: 647–651

Moore WS (1984) Radium isotope measurements using germanium detectors. Nucl. Inst. Methods 223: 407–411

Moore WS (1996) Large groundwater inputs to coastal waters revealed by ^{226}Ra enrichments. Nature 380: 612–614

Moore WS (1999) The subterranean estuary: A reaction zone of ground water and sea water. Marine Chem. 65: 111–126

Moore WS (2000) Determining coastal mixing rates using radium isotopes. Cont. Shelf. Res. 20: 1993–2007

Moore WS & Ralph Arnold (1996) Measurement of ^{223}Ra and ^{224}Ra in coastal waters using a delayed coincidence counter. J. Geophys. Res. 101: 1321–1329

Moore WS & Shaw TJ (1998) Chemical signals from submarine fluid advection onto the continental shelf. J. Geophys. Res. 103: 21543–21552

Moore WS, Krest J, Taylor G, Roggenstein E, Joye S & Lee R (2002) Thermal evidence of water exchange through a coastal aquifer: Implications for nutrient fluxes, Geophys. Res. Letters, 29: 10.1029/2002GL014923

Reid DF & Sackett WM (1982) Radium in the near-surface Caribbean Sea. Earth Planet. Sci. Lett. 60: 17–26

Rasmussen LL (1998) Groundwater Flow, Tidal Mixing, and Haline Convection in Coastal Sediments. Masters Thesis, Florida State University, Tallahassee, FL

Rasmussen LL, Chanton JP, Meacham SP, Furbish DJ & Burnett WC (in press) Groundwater flow, tidal mixing, and haline convection in coastal sediments: Field and modeling studies. Cont. Shelf Res.

Rutkowski CM, Burnett WC, Iverson RL, Chanton JP (1999) The Effect of groundwater seepge on nutrient delivery and seagrass distribution in the northeastern Gulf of Mexico. Estuaries 22: 1033–1040

Shaw TJ, Moore WS, Kloepfer J & Sochaski MA (1998) The flux of Barium to the coastal waters of the southeastern United States: The importance of submarine groundwater discharge. Geochim. Cosmochim. Acta 62: 3047–3052